https://doi.org/10.5194/egusphere-2024-2418
Preprint. Discussion started: 15 August 2024

Hillslope diffusion and channel steepness in landscape evolution models

David G. Litwin[1], Luca C. Malatesta[1], and Leonard S. Sklar[2]

[1]Earth Surface Process Modelling, Helmholtz Center GFZ Potsdam, Potsdam, Germany
[2]School of Environmental Science, Simon Fraser University, Canada

Correspondence: David G. Litwin (david.litwin@gfz-potsdam.de)

Abstract. The streampower fluvial erosion (SP) model is the basis for many analyses and simulations of landscape evolution. It assumes that the rate of river incision into bedrock depends only on flow intensity and rock erodibility, and is insensitive to sediment flux. In two dimensions, the SP model is often coupled with diffusion processes, which together describe the coupled evolution of channels and hillslopes (SPD models). While it is implicitly assumed that channels in the SPD models retain their detachment-limited character, this has not been extensively tested. Here we show that the deposition component of hillslope diffusion has a substantial effect on channel slope and relief in SPD models, and present a new method to predict the channel steepness index from model parameters. We contrast the results with those of a mixed bedrock-alluvial river model coupled with a hillslope diffusion model that both track sediment mass balance, and suggest that the combination of mass-conservative hillslope processes and non-mass-conservative fluvial erosion in SPD models leads to unrealistic scaling behavior. We demonstrate this by examining several field sites where an SPD model adequately describes the spacing of first-order valleys, and show that it is inadequate to predict channel steepness.

1 Introduction

Detachment limited erosion models are widely used to simulate and interpret how climate and tectonics affect bedrock river long profiles. Such models assume that rivers evolve only to erode bedrock, and sediment does not affect the rate of incision (Sklar and Dietrich, 1998). Detachment limited erosion models may be formulated in terms of excess shear stress (Whipple and Tucker, 1999; Howard and Kerby, 1983), or streampower (Seidl and Dietrich, 1992; Howard, 1994). In either case, such assumptions reduce to a common model form, in which fluvial erosion is proportional to the product of discharge (often replaced with drainage area) to a power, and slope to a power. Here we refer to this type of model as the streampower (SP) model.

Extending the SP model from channel long profiles to two dimensions requires consideration of erosion processes not driven by concentrated water flow, collectively called hillslope processes. Hillslope processes are most often represented by a conservation law in which the sediment flux varies (linearly or nonlinearly) with slope, making them diffusional processes. Combined ‘streampower plus diffusion’ (SPD) models have become the tool of choice for a wide range of geomorphologic problems, from constraining site-specific erosion (Barnhart et al., 2020b), to identifying controls on drainage reorganization

https://doi.org/10.5194/egusphere-2024-2418
Preprint. Discussion started: 15 August 2024

(Lyons et al., 2020), the evolution of orogens (Wolf et al., 2022) and explaining erosion rates globally (Ruetenik et al., 2023). Others have added complexity to the hydrological processes used to generate discharge, but have maintained the SPD erosion form to simulate the evolution of small watersheds (Litwin et al., 2022, 2024) and entire continental orogens (Shen et al., 2021).

SPD models are nonlinear advection-diffusion equations, which have been been used to explain controls on drainage density and the spacing of first order valleys (Perron et al., 2008, 2009; Theodoratos et al., 2018; Theodoratos and Kirchner, 2020; Bonetti et al., 2020). Less has been done to understand the effects of hillslope processes on channel profiles in SPD models. This is perhaps because theoretical studies have generally recognized that SPD models should only apply to small domains, where it is conceivable that no redeposition of fluvial sediment occurs (e.g., Perron et al., 2008; Bonetti et al., 2020). SPD models are applied beyond this scope. In such cases, diffusion is sometimes included simply to reduce slope and elevation near drainage divides, where the SP model alone predicts that channel elevation goes to infinity as area goes to zero. The implicit assumption is that the effect of diffusion is confined to headwaters, such that channels in SPD models remain detachment limited and their dynamics independent of sediment flux. However, it has long been known that the effect of diffusion can persist through the entire drainage network. Howard (1994) showed one parameter combination for which the SPD model produced increased channel slope compared to the SP model prediction at large drainage areas. Persistent increases in slope, integrated over a basin, lead to a substantial difference in total relief as well. This feature has not received widespread attention, nor have its implications for the growing number of applications of SPD models been explored.

The goal of this paper is to investigate how hillslopes affect channel profiles in SPD models, and determine whether these effects meaningfully change how SPD model results should be interpreted. We show that hillslope diffusion can strongly affect steady-state channel steepness, and demonstrate a new way in which this effect can be predicted directly from model parameters when diffusion is linear (the 'SPLD' model). We discuss the physical interpretation of the channel-hillslope coupling in SPD models, focusing on the effect of mixing mass-conserving and non-mass-conserving process models while not distinguishing sediment from bedrock. We contrast the SPD model predictions with a mass-conserving model of hillslopes and mixed bedrock-alluvial rivers which shows less sensitivity to local hillslope processes. Lastly, we examine several field sites where the SPLD model can correctly predict the spacing of first order valleys, and demonstrate that it is inadequate to predict channel steepness.

2 Theory and Methods

2.1 Streampower law and channel steepness

The basic SP model for the evolution of channel elevation z with along-channel distance x is:

$$\frac{\partial z}{\partial t} = -KA^m S^n + U \tag{1}$$

where t is time, K is the streampower incision coefficient, $A(x)$ is the upslope area $S(x)$ is the channel slope, U is the uplift or baselevel change, and m and n are the area and slope exponents of the streampower law. At steady state, the SP model predicts

https://doi.org/10.5194/egusphere-2024-2418
Preprint. Discussion started: 15 August 2024

a power law relationship between slope and area:

$$S = k_{sn} A^{-m/n} \tag{2}$$

$$k_{sn,pred} = (U/K)^{1/n} \tag{3}$$

where k_{sn} is the normalized steepness index, and $k_{sn,pred}$ is the predicted steepness based on the SP model. Independent of model form, k_{sn} can be estimated directly from regression of log-transformed slope and area using (2). Alternatively, it can be estimated from regression of elevation and the area-normalized distance coordinate χ, which minimizes noise that arises from the elevation derivative (Perron and Royden, 2013):

$$z(x) = z(x_b) + \left(\frac{U}{K A_0^m}\right)^{1/n} \chi \tag{4}$$

$$\chi = \int_{x_b}^{x} \left(\frac{A_0}{A(x)}\right)^{m/n} dx \tag{5}$$

where x_b is an arbitrary baselevel location, and A_0 is a reference drainage area. The slope of the relationship between χ and z reduces to $k_{sn,pred}$ when A_0=1. In order for χ to have units of [L], A_0 should have units of [L^2], in which case $k_{sn,pred}$ would be dimensionless. However here we always report k_{sn} according to Equation 3, which has SI units of m$^{2m/n}$. The numerical value will be the same as if A_0=1 m^2.

2.2 Streampower plus linear diffusion (SPLD) model

The SPLD model generalizes the SP model to two dimensions and adds a linear diffusion term to describe hillslope sediment transport:

$$\frac{\partial z}{\partial t} = -K A^m |\nabla z|^n + D\nabla^2 z + U, \tag{6}$$

where D is the hillslope diffusivity. In two dimensions, we can also write a constraint that describes the relationship between elevation and the specific area a (e.g., Bonetti et al., 2020, Eq. 5):

$$-\nabla \cdot \left(a \frac{\nabla z}{|\nabla z|}\right) = 1. \tag{7}$$

The specific area is the intrinsic counterpart of drainage area, defined as the drainage area per unit contour width in the limit that the contour width is small. Because it is an intrinsic property of the topographic surface, replacing area with the specific area in (6) produces a governing equation that is independent of grid resolution (Bonetti et al., 2020). (Bonetti et al., 2018) describe a way to estimate a by integration of the contour curvature, but for numerical landscape evolution simulations in which a is recalculated many times, it is more efficient to estimate $a = A/v_0$ from an algorithmic solution for drainage area A and grid cell width v_0. For this reason it will be helpful to write (6) explicitly accounting for the grid cell width, as in Litwin et al. (2022):

$$\frac{\partial z}{\partial t} = -K v_0^m a^m |\nabla z|^n + D\nabla^2 z + U. \tag{8}$$

https://doi.org/10.5194/egusphere-2024-2418
Preprint. Discussion started: 15 August 2024

2.3 Model setup

We ran simulations on raster grids using the open source Earth surface modelling platform Landlab (Hobley et al., 2017; Barnhart et al., 2020a). Fluvial erosion is calculated using an implicit scheme with D8 flow routing based on Braun and Willett (2013). Linear diffusion is calculated using an explicit finite volume scheme. The two processes (plus the source term U) are loosely coupled to calculate total topographic change in each timestep. While the SPD models have been solved simultaneously (e.g., Perron et al., 2008), loosely coupled schemes are far more common (Tucker et al., 2001; Barnhart et al., 2018; Bovy and Lange, 2023).

All SPLD model results use a domain size of 200x400 cells, while the actual domain length varies with the grid cell width. The top and bottom edges are fixed-elevation boundaries, and the left and right are zero-flux boundaries. All model runs use the same initial condition: a randomly seeded rough surface with a mean elevation of 20 cm. We run simulations for 250 t_g (the characteristic SPLD timescale, see Appendix A), at which point all simulations show negligible change in relief with time. We used Landlab to calculate the χ-coordinate for locations with drainage areas greater than 100 cells. This threshold was chosen to ensure the analysis is conducted on relatively large channels with linear relationships between χ and elevation. More complex schemes could be devised to estimate the threshold for what is a channel (Passalacqua et al., 2010; Clubb et al., 2014), but we found little variation in our results for different threshold values, once the threshold is sufficiently large. We estimated the normalized steepness index from χ and elevation using linear regression.

3 Results

3.1 Hillslope diffusion increases channel steepness

Stream channels extracted from steady-state results of the SPLD model have higher normalized steepness k_{sn} and relief than predicted by the SP model. Figure 1(a) shows one simulation with well-developed fluvial dissection where K=5e-5 yr^{-1}, D=0.011 m^2/yr, U=0.0005 m/yr, m=0.5, n=1, and v_0=20 m. Differences between SP and SPLD channels are visualised in three ways. In the inset plot of Figure 1(a), an extracted channel profile is compared with the profile that would be expected from the 1D SP model with the same K, U, m, n, and upslope area. In this particular channel, SPLD relief is nearly twice that of the equivalent SP model. The increase in k_{sn} is also apparent from the intercept of log-scaled slope and area (Figure 1(b)) and slope of the χ-elevation relationship (Figure 1(c)). Both show near doubling of k_{sn} in comparison to the SP model prediction.

The SPLD channel steepness varies systematically with model parameters. Figure 2 shows variation with diffusivity and grid cell width (colors) for different values of the predicted SP channel steepness $k_{sn,pred}$, and different combinations of m and n. The value of $k_{sn,pred}$ differs with the streampower incision coefficient K. Increasing diffusivity alone increases the SPLD channel steepness in nearly all cases, but the sensitivity depends on other parameters. When $k_{sn,pred}$ is small (when K is large), SPLD channel steepness is closer to the predicted SP value. The sensitivity of k_{sn} to diffusivity is greatest when the

https://doi.org/10.5194/egusphere-2024-2418
Preprint. Discussion started: 15 August 2024

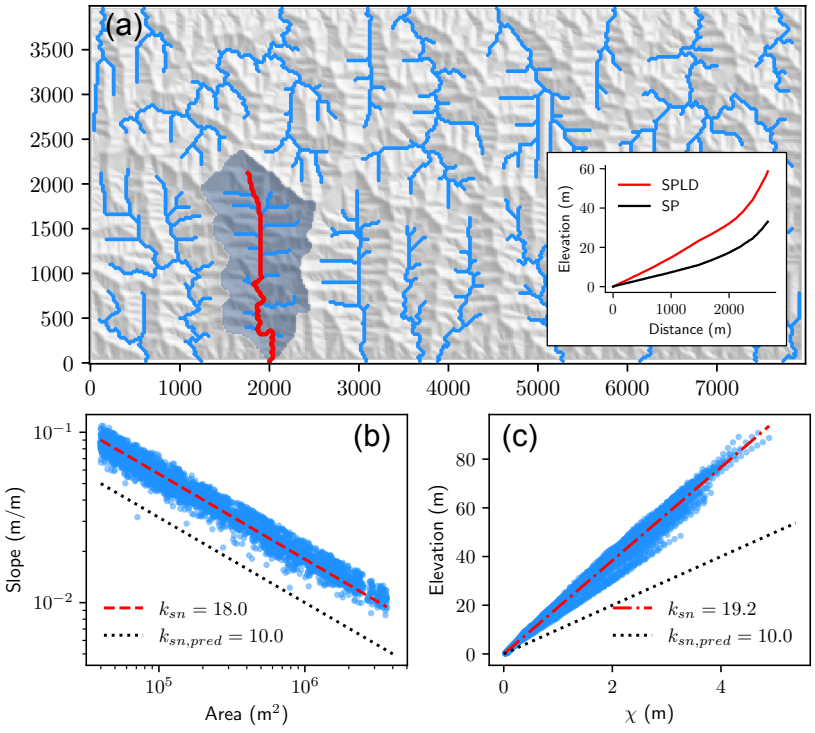

Figure 1. Visualizing the increase in channel steepness associated with hillslope processes for model simulation with K=5e-5 yr^{-1}, D=0.011 m^2/yr, U=0.0005 m/yr, m=0.5, n=1, and v_0=20 m. (a) Hillshade of steady state topography, where channels with drainage area > 100 cells are highlighted in blue. Inset plot shows the profile of the channel highlighted in red compared with expected without hillslope processes (black). The basin has approximately twice the relief of that without hillslope processes. (b) Increase in slope at a given area for all channels, compared to the prediction from the SP model ($k_{sn,pred}$). (c) Increase in channel elevation relative to expectation from χ-coordinate in comparison to the prediction from the SP model. The units of k_{sn} are m$^{2m/n}$.

fluvial incision is weakly sensitive to slope (m=0.4, n=0.6), even despite the fact that the corresponding K values are larger compared to the other streampower exponent cases.

SPLD channel steepness also increases with the grid cell width v_0. When the grid cell width is large, the channel steepness can remain close to the SP model prediction, though this diminishes as K becomes large or D becomes small. Several works have already addressed the grid cell dependence of the SPLD model (Howard, 1994; Perron et al., 2008; Pelletier, 2010; Hergarten, 2020; Hergarten and Pietrek, 2023). As others have already noted (e.g., Hergarten and Pietrek, 2023), the combination of fluvial erosion and hillslope diffusion is the source of the grid cell dependency of the SPLD model.

We can compensate for the grid cell dependence of the SPLD model by holding the quantity Kv_0^m constant when varying v_0 (Bonetti et al., 2020). Holding this term constant implies that at different grid cell widths, we need different values of the SP

https://doi.org/10.5194/egusphere-2024-2418
Preprint. Discussion started: 15 August 2024

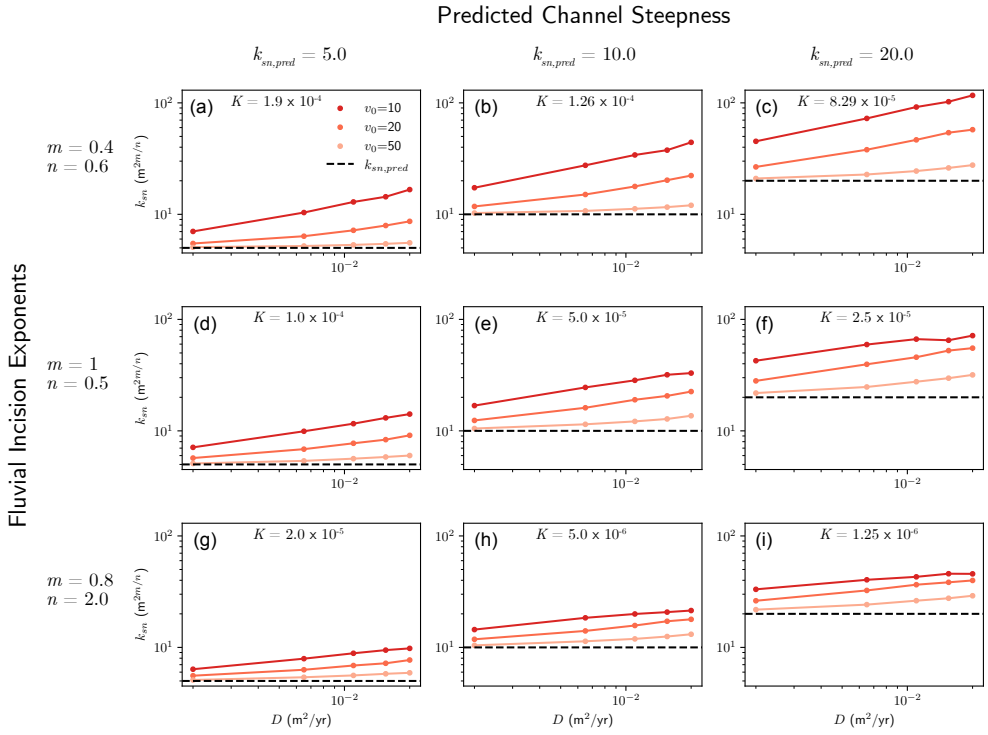

Figure 2. Increase in steady-state normalized channel steepness from the SPLD model with hillslope diffusivity D and grid cell width v_0 (colors) for three values of the predicted SP channel steepness $k_{sn,pred}$ (columns) and three combinations of the streampower exponents m and n (rows). Subplots have different values of K according to the combination of n and $k_{sn,pred}$ (Equation 3). The uplift rate U is held constant. The units of v_0 are meters, and the units of K are m^{1-2m}/yr.

steepness $k_{sn,pred} = (U/K)^{1/n}$ in order to achieve the same SPLD steepness, expressed in the relationship between slope and area or χ and elevation. We define a new steepness quantity, the specific area steepness k_{snap} that will remain constant even while $k_{sn,pred}$ varies, beginning with the 1D streampower law at steady state:

$$0 = -Kv_0^m a^m S^n + U \tag{9}$$

$$S = \left(\frac{U}{Kv_0^m}\right)^{1/n} a^{-m/n}. \tag{10}$$

Where again a is the specific area. Then the specific area steepness is the coefficient on slope:

$$k_{snap} = \left(\frac{U}{Kv_0^m}\right)^{1/n}. \tag{11}$$

Figure 3 shows that keeping Kv_0^m constant does reduce the dependence of the results on the grid spacing, but does not eliminate it in all cases. Even when the relative change in steepness with grid size is small (3(c)), the results are still sensitive

https://doi.org/10.5194/egusphere-2024-2418
Preprint. Discussion started: 15 August 2024

to diffusivity D, suggesting this is a characteristic feature of the SPLD model. More work could be done to further explore the scaling analysis with the specific area version of the model, but as we will show in the discussion, there are reasons to be generally skeptical of the physical realism of the scaling that emerges from the SPLD model with or without grid dependence correction.

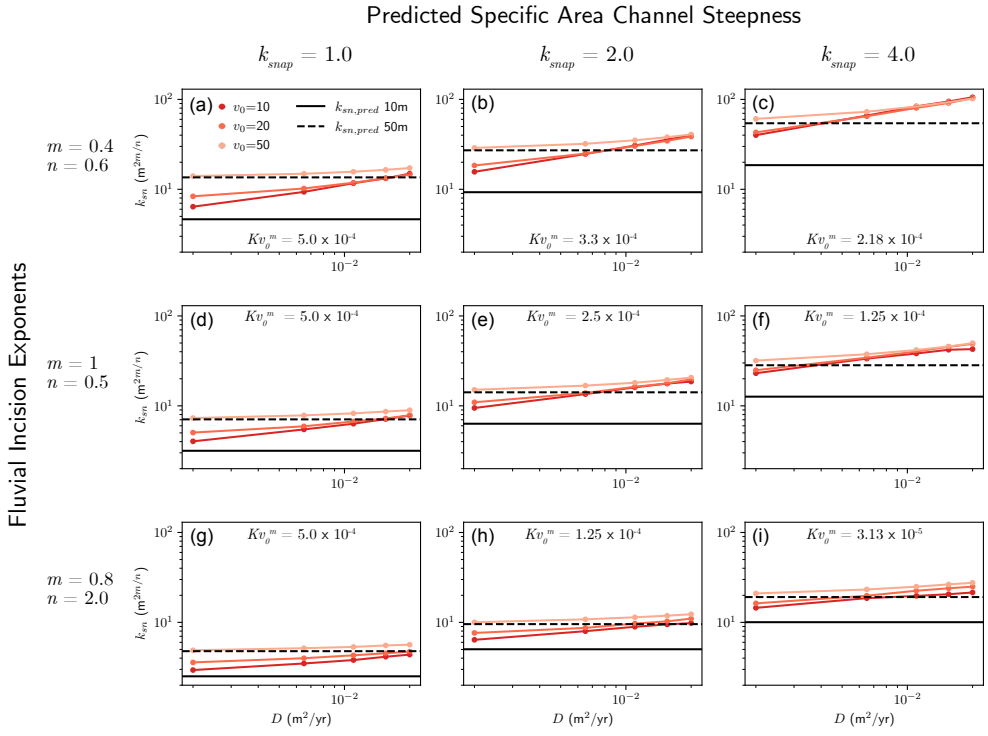

Figure 3. Variation of channel steepness k_{sn} with D and v_0 for several values of the specific area steepness k_{snap}, as defined in Equation 11, and three different combinations of m and n. Curves with different values of v_0 have different $k_{sn,pred}$ in order to conserve the quantity Kv_0^m within each subplot. We show the largest $k_{sn,pred}$ (for v_0=50 m) and the smallest (for v_0=10 m) for reference.

3.2 Prediction and scaling of SPLD channel steepness

The channel steepness of the SP model can be derived directly from rearranging the SP model (Equation 3), however, no equivalent solution exists for the SPLD model. In theory, the SPLD steepness can be derived by rearranging Equation 6 for the relationship between slope and drainage area:

$$S = \left(\frac{U + D\nabla^2 z}{K} \right)^{1/n} A^{-m/n}. \tag{12}$$

This shows that in channels, where Laplacian curvature is positive, there is net deposition of material eroded from hillslopes so the steepness must be greater than in the SP model alone (Equation 3). This is what we have seen in Figures 1 and 2. We

https://doi.org/10.5194/egusphere-2024-2418
Preprint. Discussion started: 15 August 2024

can quantify this difference by plotting the diffusion term relative to uplift. Figure 4(a) shows this for part of the watershed highlighted in Figure 1, revealing that the deposition in valley bottoms locally increases the effective uplift rate by a factor of two.

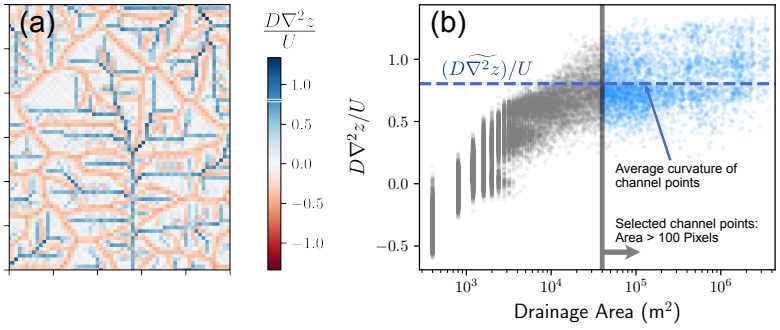

Figure 4. (a) The diffusion term relative to uplift for part of the highlighted watershed shown in Figure 1. In valley bottoms, the diffusion term is net depositional, and is nearly equal to the uplift rate. (b) The diffusion relative to uplift versus drainage area, showing that they are not strongly correlated for large drainage areas. Points colored in blue have drainage area $>$ 100 cells, and a mean value shown with a dashed blue line. The mean line also appears on the colorbar of (a).

We can generalize the insight from pointwise calculations of the diffusion relative to uplift to explain the difference between simulated steepness and predicted steepness of the SP model. We do this by taking an average of the diffusion term over channelized cells, which is possible because the hillslope flux divergence is generally poorly correlated with drainage area once drainage area is large (Figure 4(b)), even while the relationship between the diffusion term and streampower term remains linear to balance uplift (Theodoratos et al., 2018). We denote the mean for locations with drainage area $>$ 100 cells with ($\sim$), such that $(D\widetilde{\nabla^2 z})/U$ is the mean diffusion relative to uplift in these locations.

An analytical relationship between $(D\widetilde{\nabla^2 z})/U$ and the steepness deviation $(k_{sn}/k_{sn,pred})^n - 1$ can be derived (Appendix B), following similar logic to Equation 12. Note that the steepness deviation reduces to the relative error formula $(k_{sn} - k_{sn,pred})/k_{sn,pred}$ when n=1. Figures 5(a, d, g) show that the mean hillslope diffusion term relative to uplift in channels predicts the steepness deviation well for model runs in Figure 2. Each subplot in Figure 5 aggregates all values of K, D, and v_0 shown in rows of Figure 2. Most points fall very close to the 1:1 line, while some points with large average diffusion in channels have lower than expected steepness deviation. These cases have relatively low dissection, and it is assumed that model boundary conditions are at this point beginning to affect the relief and channel steepness.

While these results confirm a simple rearrangement of the governing equation, the channel curvature $\widetilde{\nabla^2 z}$ is generally not known prior to simulation. To estimate the steepness deviation from the model parameters alone, we make use of scaling analyses of the governing equations of the SPLD model. Litwin et al. (2022) presented a dimensional analysis of equations (7, 8) for the case m=0.5, n=1 that defines characteristic scales for horizontal length ℓ_g, height h_g, and time t_g. In Appendix A we

https://doi.org/10.5194/egusphere-2024-2418
Preprint. Discussion started: 15 August 2024

show the same analysis for any values of the exponents m and n. Critical to our analysis here is the characteristic horizontal length scale, which quantifies the distance from the ridge at which there is a transition from relative importance of diffusive to advective processes. The characteristic scale ℓ_g is analogous to the SPLD horizontal length scale derived by Perron et al. (2009) and Theodoratos et al. (2018), which we call ℓ_c, only ℓ_g comes from the version using specific area a (Equations 7, 8) and ℓ_c comes from the version using area A (Equation 6):

$$\ell_g = \left(\frac{D^n U^{1-n}}{K v_0^m} \right)^{1/(m+n)} \tag{13}$$

$$\ell_c = \left(\frac{D^n U^{1-n}}{K} \right)^{1/(2m+n)} . \tag{14}$$

The relationships in Figure 4 showed that the channels were steeper in comparison to the SP model prediction when diffusive processes were stronger relative to advective processes, and that steepness was also inversely proportional to the grid cell width. These results also hold for those where $K v_0^m$ was held constant, because the underlying solution is the same. Using the characteristic scales, we found ℓ_c (Equation 14) normalized by v_0 is not only proportional to the steepness deviation $(k_{sn}/k_{sn,pred})^n - 1$, but is approximately equal to it (Figure 5(b, e, h)). In the SPLD model ℓ_c is an important control on the spacing of first order valleys (Perron et al., 2009); it appears to be an important control on channel steepness in the model as well.

The length scale ℓ_g (Equation 13) derived for the SPLD model with specific area performs slightly better overall (Figure 5(c, f, i). This scaling holds for different values of m and n, though there appears to be a slight vertical offset of the curves relative to the 1:1 line depending on the particular parameter values. The root mean squared error (RMSE) and log-transformed RMSE (RMSLE) suggest ℓ_c/v_0 and ℓ_g/v_0 are comparable predictors, but visual inspection suggests the trend in steepness deviation with ℓ_g/v_0 is more aligned with the steepness deviation than ℓ_c. This is likely related to the dependence of ℓ_g on v_0. The ratio ℓ_c/v_0 implies scaling of the steepness deviation with v_0^{-1}, while using ℓ_g/v_0 implies scaling with $v_0^{-(2m+n)/(m+n)}$.

The scaling results suggest there is an inherent trade off in the SPLD model. Studies have chosen ℓ_c/v_0 or ℓ_g/v_0 to be greater than one in order to resolve the diffusive-to-advective transition that occurs with distance downstream from ridges (Theodoratos et al., 2018; Litwin et al., 2022). When equal to one, SPLD steepness is already double the SP steepness, when n=1. This may reflect actual channel-hillslope coupling (we will discuss this further in the next sections), but it may also lead to unexpected behavior. For instance, if K and D are both increased for a simulation where lithology is perceived to be softer and more weatherable, the steady state relief may in fact increase (according to the scaling in Figure 5).

In contrast, if one chooses parameter values such that ℓ_c/v_0 or ℓ_g/v_0 is small, hillslopes will not be fully resolved, and numerical diffusion, rather than the explicit hillslope diffusion, becomes important. For some large-scale applications, this may be fine, as it satisfies the need to prevent elevation from going to infinity as drainage area goes to zero. In any case, understanding how the channel-hillslope coupling will affect the simulated results should be an important part of SPLD model use, especially for understanding how the results contrast with intuitions developed from the SP model.

Finally, while we have focused on coupling the SP model with linear diffusion, the scaling has explanatory power for nonlinear diffusion as well. When we run simulations with the same parameter values shown in Figures 2 and 4, but replace

https://doi.org/10.5194/egusphere-2024-2418
Preprint. Discussion started: 15 August 2024

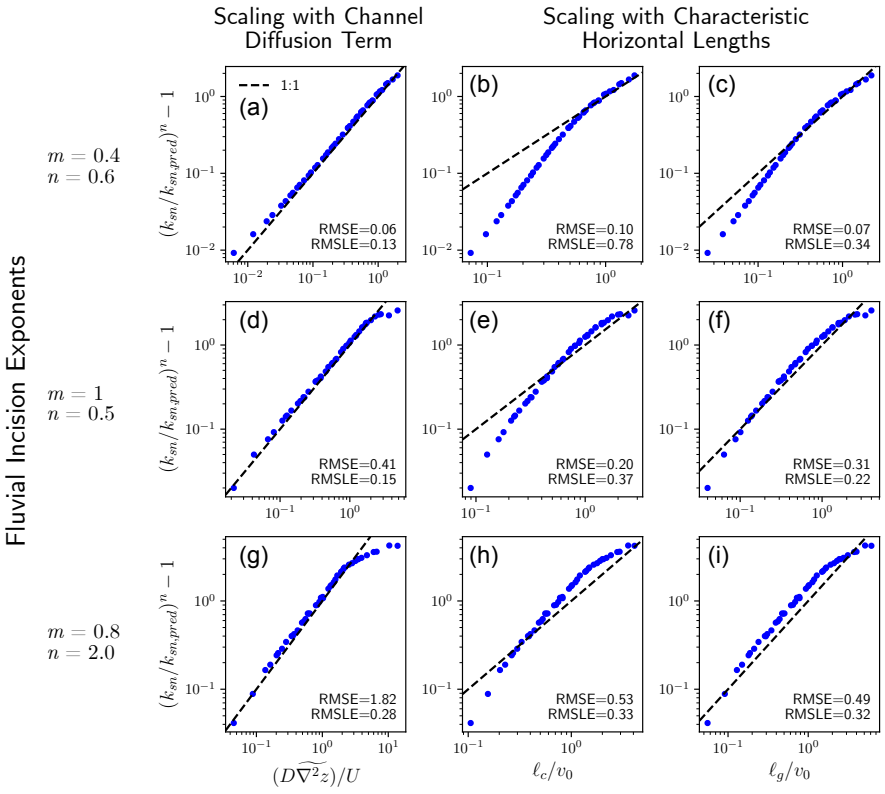

Figure 5. (a, d, g) The average of the diffusion term in channels relative to uplift (See Figure 4) versus the steepness deviation. Each subplot in a row contains points from all columns in the corresponding row of Figure 2. (b, e, h) The length scale ℓ_c (Equation 14) relative to the grid cell width explains the steepness deviation. (c, f, i) The length scale ℓ_g (Equation 13) relative to the grid cell width explains the steepness deviation. RMSE is the root mean squared error and RMSLE is the root mean squared log error.

linear diffusion with the nonlinear diffusion model proposed by Ganti et al. (2012) with a critical slope of 0.5, we find that simulated channels tend to fall at or above the 1:1 line (Figure 6). That is, nonlinear diffusion increases channel steepness relative to the SP solution at least as much as suggested by the SPLD scaling.

4 Discussion

4.1 Physical interpretation of SPLD channel-hillslope coupling

The results we have presented demonstrate a fairly simple concept: hillslope sediment flux to channels increases channel steepness in the SPLD model, and that this scales with the activity of hillslope processes relative to fluvial processes. Is this effect physically reasonable? Mechanistic models have attributed a component of channel slope to sediment transport (Sklar

https://doi.org/10.5194/egusphere-2024-2418
Preprint. Discussion started: 15 August 2024

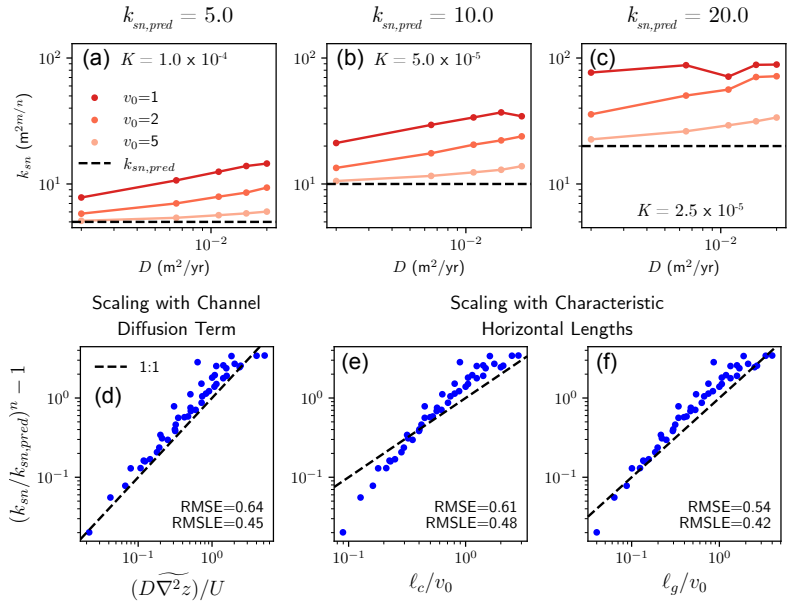

Figure 6. (a, b, c) Increase in steady-state normalized channel steepness from the SPLD model with hillslope diffusivity D and grid cell width v_0 (colors) for three values of the predicted SP steepness $k_{sn,pred}$. Diffusion is a nonlinear, second-order Taylor expansion of the critical slope model (Ganti et al., 2012) and the critical slope is 0.5. All results shown have $m = 0.5$ and $n = 1.0$. The units of v_0 are meters, and the units of K are m^{1-2m}/yr. Compare with Figure 2(d, e, f), which has the same parameters but uses linear diffusion. (d, e, f) Scaling relationships at steady state. (d) The diffusion term relative to uplift averaged over channels ($\sim$) versus the steepness deviation. Most sites have steepness deviation greater than or equal to that suggested by the linear diffusion analytical solution. (e) The deviation explained with the characteristic length scales ℓ_c from Theodoratos et al. (2018), and (f) ℓ_g from Litwin et al. (2022). Compare with Figure 5(d, e, f).

and Dietrich, 2006), and field studies have shown that resistive hillslope sediment can affect channel steepness (Johnson et al., 2009; Finnegan et al., 2017; Lai et al., 2021). How do these observations relate to that found in the SPLD model?

To understand channel-hillslope coupling in the SPLD model, it is first important that the same fluvial and hillslope processes operate at every cell. This has been described with the sub-grid concept that each cell contains one segment of channel and adjacent hillslopes, though models do not explicitly resolve such sub-grid features (Howard, 1994). Conceptually, the cell elevation is then the average of the channel and hillslope component elevations. Hergarten (2020) describes that the hillslope flux may be effectively only distributed on the hillslope components of the cell (Perron et al., 2008; Howard, 1994) or only across on the channel component (Pelletier, 2010) in order to reduce scale dependence of the model. Assuming that channels must ultimately transport hillslope material to maintain mean cell elevation at steady state, the two sub-grid representations still have the effect that sediment must be removed before erosion can begin to counter uplift.

https://doi.org/10.5194/egusphere-2024-2418
Preprint. Discussion started: 15 August 2024

In this sense, the SPLD model channel-hillslope coupling is a kind of sediment cover effect. However, because the SPLD model couples mass conserving hillslope diffusion with non-mass-conserving fluvial erosion, this cover effect is strictly local. That is, while using a spatially and temporally uniform K implies sediment is as difficult to erode as bedrock, the eroded material cannot deposit and does not continue to affect conditions downstream. Past studies have argued that this is appropriate for applications where the domain of interest is small enough that re-deposition can be ignored and where sediment has similar erodibility to bedrock (Perron et al., 2008). However, the SPLD model has been used in scaling analyses and applications at much larger scales (Theodoratos et al., 2018; Theodoratos and Kirchner, 2020; Wolf et al., 2022; Shen et al., 2021). The question of applicability at small scales is also in doubt. In reality, there is sediment retained at every scale in the fluvial system, and such sediment retention can affect channel properties even in headwaters (Sklar, 2024). Furthermore, cases where the travel distances of sediment particles are long are also likely to have finer grain sizes and consequently a higher erodibility of sediment relative to bedrock, making the combination of features of the SPD model unlikely.

Because of the combination of mass conserving and non-mass-conserving processes, the SPLD model predicts that channel steepness should be correlated with hillslope length (Hergarten, 2020). In this study, we have shown that the SPLD model predicts this effect persists in downstream channels. In the following sections we investigate both the effect of sediment conservation and the implied scaling between steepness and hillslope length.

4.2 Distinguishing eroded materials and conserving sediment mass

While we have focused on the variety of SPD models that track only the topographic elevation, early numerical models recognized the importance in distinguishing bedrock and sediment fluvial erodibility (Howard, 1994; Tucker et al., 2001). This type of modeling continues today (e.g., Egholm et al., 2013; Roy et al., 2016; Campforts et al., 2020), but for many applications SPD models that track only topography became the default because they use minimal complexity to capture first-order features of fluvial topography, and can be highly computationally efficient (Braun and Willett, 2013).

If the aim of a particular application is to work in two dimensions but maintain channel steepness and relief estimated by analysis of channel long profiles (e.g., Harel et al., 2016), one solution would be to prevent deposition by diffusion, as in Campforts et al. (2017). This still allows diffusion to limit steady state elevation as area goes to zero, but eliminates most of the capacity of diffusive processes to balance advection. If drainage density is an important model target, this will not be effective solution.

One can regain some of the realism of separating bedrock and sediment, but maintain some of the simplicity of the stream-power model, using models like the Stream Power with Alluvium Conservation and Entrainment (SPACE, Shobe et al., 2017) model coupled with hillslope diffusion. SPACE explicitly tracks sediment mass balance and captures the reduction in bedrock incision due to sediment cover. It has steady-state analytical solutions for channel slope in mixed bedrock-alluvial conditions (Appendix C) to which we can compare the numerical results of SPACE coupled with diffusion.

We considered three different variables from SPACE: K_s is the streampower coefficient for sediment, K_r is the coefficient for bedrock, and F_f is the fraction of fine sediment, which determines how much of the sediment that is entrained will remain in suspension and leave the mass balance. All simulations were run on 100x100 grids with three zero flux boundaries and one

https://doi.org/10.5194/egusphere-2024-2418
Preprint. Discussion started: 15 August 2024

fixed value boundary on the lower edge. We used 30 m grid cell width, 25 yr timesteps, for 2 Myr. We set m=0.5, n=1.0, U=0.5 m/kyr, D=0.05 m^2/yr, and K_r=0.1 kyr^{-1}. All additional SPACE parameters were held constant, and are given in Appendix C. We assumed all material deposited by hillslope diffusion has the same properties as sediment produced by bedrock erosion. This is the same approach that Shobe et al. (2017) used in a 2D demonstration.

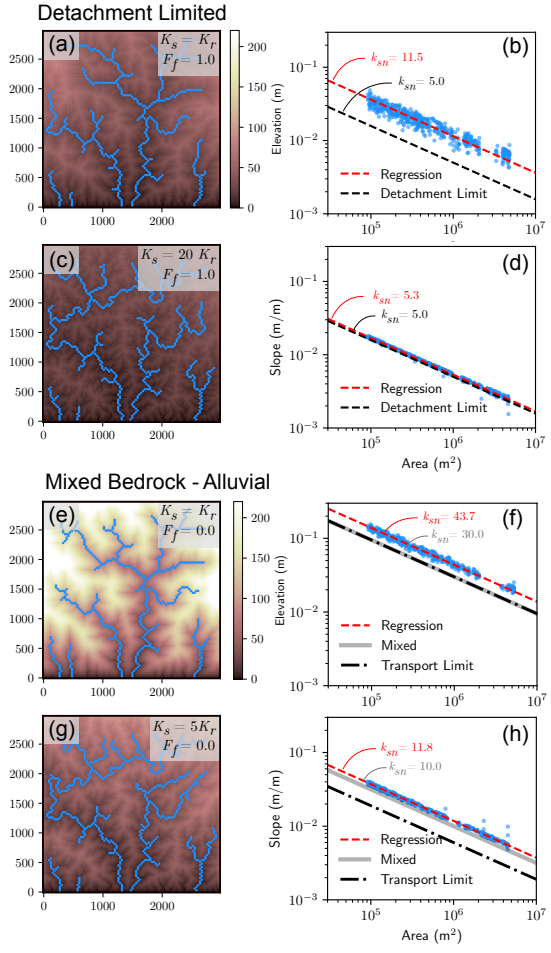

Figure 7. 'SPACE plus linear diffusion' model results, showing elevation with locations where drainage area > 100 cells highlighted in blue (left column) and slope-area relationships (right column). (a, b) Case most similar to SPD model. (c, d) Same as (a, b), but sediment much more erodible than bedrock. (e, f) All sediment remains in mass balance (F_f=0), lines of comparison are for 1D mixed bedrock+alluvial solution and transport limit. (g, h) Same as (e, f) but sediment is more erodible than bedrock. The "Detachment limit" solution is the same as the SP model. "Transport limit" and "Mixed" solutions are located in Appendix C.

Figure 7 shows topography and channel slope-area relationships for four simulations using 'SPACE plus linear diffusion'. The first case (Figure 7(a, b)) is analogous to the SPLD model: sediment and bedrock erodibility are the same (K_s=K_r),

https://doi.org/10.5194/egusphere-2024-2418
Preprint. Discussion started: 15 August 2024

and sediment deposited by diffusion leaves the mass balance once it becomes suspended (F_f=1.0). The equilibrium channel steepness is 11.5 m, more than twice the detachment-limited prediction of 5.0 m, which is the same as $k_{sn,pred}$ when K is replaced with K_r in Equation 3. The second case (Figure 7(c, d)) is the same as the first, except we increased the erodibility of sediment (K_s=20K_r). Here, the channel steepness is 5.3 m, very close to the predicted value of 5.0 m.

Next we set F_f=0 as an end-member of 'mixed bedrock-alluvial rivers' in which the hillslope sediment supply is entirely gravel and coarser and all sediment remains in the mass balance. Field studies of hillslope sediment production and bedload fraction of total fluvial sediment flux suggest that F_f is generally at least 0.5, and up to 0.9 for gravel bedded rivers (Turowski et al., 2010). We show results for F_f=0 here because there is an analytical solution for SPACE to which we can compare the coupled channel-hillslope numerical results.

The first case with F_f=0 (Figure 7(e, f)) is otherwise the same as Figure 7(a, b). Because sediment and bedrock erodibility are equal, the analytical solutions for mixed bedrock-alluvial equilibrium steepness and transport limited equilibrium steepness are equivalent. The equilibrium steepness is 30.0 m, significantly higher than the detachment limited cases (Figures 7(b, d)), but the channels are also relatively closer to the respective analytical solution with steepness of 43.7 m. When the sediment is five times more erodible than bedrock (Figures 7(g, h)) it is clear that the channels follow the mixed bedrock-alluvial analytical solution. Here the analytical solution predicts a channel steepness of 10.0 m, and the channel steepness from regression is 11.8 m. In other words, when sediment mass is conserved, the effect of the particular diffusivity or length of adjacent hillslopes on channel slope diminishes compared to the need to transport all sediment from upstream.

Why is there still an offset between equilibrium steepness of mixed bedrock-alluvial channels and the analytical solution (Figures 7(f, h)), if sediment mass is conserved (F_f=0.0)? The residual deviation is due to the bed cover effect in SPACE. While diffusivity does not affect the total amount of sediment that must leave the watershed, it does increase the equilibrium sediment thickness in channels, which can reduce the effectiveness of incision (Shobe et al., 2017). The average channel sediment thicknesses for simulations in Figures 7(e) and 7(g) are 2.2 and 1.0 m respectively; the SPACE analytical solutions (Appendix C) for steady state thickness without diffusion are 1.8 and 0.8 m, respectively. While the mechanism by which channel steepness is affected by sediment is different in the SPACE+diffusion and SPD models, the result may be hard to distinguish in steady-state profiles. The benefit of a model such as SPACE is that the strength of the interaction between channel steepness and hillslope sediment can be explained, and its relative importance explored through model parameters. There are other benefits to using SPACE too, such as explainable sediment flux when simulating transient landscape evolution, or the ability to parameterize lithology in terms of sediment characteristics (F_f, effective settling velocity V) or climate in terms of weathering and sediment production.

In real landscapes, the effect of local sediment input from hillslopes seems to be especially important in settings with large sediment inputs from landslides. Ott et al. (2024) show that incision thresholds associated with the delivery of landslide-derived sediment to channels decreases the sensitivity of channel steepness to erosion rate in the Northern Andes. The effect of discrete two-dimensional landslides on channel long profiles is explored by Campforts et al. (2020), who also use SPACE.

These studies, and the effects we have discussed here with SPACE and the SP model focus on the importance of sediment cover in limiting erosion. However, sediment grains moving with flowing water are the necessary tools to bedrock erosion (Sklar

https://doi.org/10.5194/egusphere-2024-2418
Preprint. Discussion started: 15 August 2024

and Dietrich, 2004; Lamb et al., 2015). This effect is implicitly included in SPACE and SP models in that sediment discharge can scale with water discharge and drainage area. However, fully addressing the effect of sediment on coupled channel-hillslope evolution including the tools effect is an important direction for future landscape evolution modelling (Gasparini et al., 2004; Egholm et al., 2013; Roy et al., 2016).

4.3 Relevance to channel-hillslope coupling in the field

While field studies have shown that coarse, resistive hillslope sediment can affect channel slope (Johnson et al., 2009; Finnegan et al., 2017; Lai et al., 2021), our analysis of the SPLD suggests a more general scaling between fluvial erodibility, diffusivity and uplift (in ℓ_c and ℓ_g) and channel steepness. Our demonstration with the SPACE model showed that this relationship is easily weakened or eliminated by differentiating sediment and bedrock erodibility, or conserving sediment mass. To explore the ℓ_c-channel steepness relationship with field data we need independent ways to assess channel steepness and the expected steepness in the absence of hillslope processes $k_{sn,pred} = (U/K)^{1/n}$. Otherwise the value of K in ℓ_c would already reflect potential influences of hillslope sediment. However, most studies only estimate $(U/K)^{1/n}$ from channel steepness (e.g., Harel et al., 2016).

One exception is the method derived by Perron et al. (2009) to estimate D/K from topography when n=1, by introducing the solution for diffusivity from hilltop curvature $U/D \approx \nabla^2 z_h$ into the SPLD model (6):

$$\frac{|\nabla z|}{\nabla^2 z - \nabla^2 z_h} = \frac{D}{K} A^{-m}, \tag{15}$$

from which they estimated m and D/K by least squares regression. Because the model used to derive (15) assumes n=1, we can estimate the predicted channel steepness $k_{sn,pred}$:

$$k_{sn,pred} = \frac{U}{K} = \frac{D}{K}\frac{U}{D} \approx \frac{D}{K}\nabla^2 z_h. \tag{16}$$

The approximation in the hilltop curvature relationship is due to the conversion of rock to regolith, which have different bulk densities. Typical ratios of rock to regolith bulk density are 1.5–2 (Roering et al., 2007; Heimsath et al., 1997). However, if the bulk density of the material eroded by fluvial processes is equal to that of bedrock, as assumed in the SP model, then U and K have the same the bulk density prefactors and the conversions cancel. Consequently the last term of Equation 16 is exactly equal to $k_{sn,pred}$ (see Appendix D).

We applied this method to several sites where Perron et al. (2009) showed that the length scale ℓ_c (their L_c) derived from (15) correlated with the spacing of first order valleys, and examine whether the sites also support the SPLD model prediction that channel steepness should also scale with ℓ_c. Assuming a uniform K, D, and U, we can compare $k_{sn,pred}$ in Equation 16 to the steepness of larger channels adjacent to the first order valleys that were the focus of Perron et al. (2009), to match our approach with the SPLD model results.

We forgo direct assessment of the SPLD scaling and calculation of ℓ_g, ℓ_c/v_0, or ℓ_g/v_0 because of dependence on the grid cell width. These are model dependent quantities whose real-world interpretation is more nebulous. For this case study we focus on general scaling expected from the SPLD model: channel steepness relative to $k_{sn,pred}$ should increase with ℓ_c.

https://doi.org/10.5194/egusphere-2024-2418
Preprint. Discussion started: 15 August 2024

Perron et al. (2009) considered five sites with varying valley spacing. We eliminated the two sites with the smallest spacing, because the first order channels do not share baselevel with higher order rivers. We estimated channel steepness from least squares regression of the χ-elevation relationship, where χ was calculated using the concavity index from Perron et al. (2009) so that the resulting channel steepness will be comparable with $k_{sn,pred}$ in Equation 16.

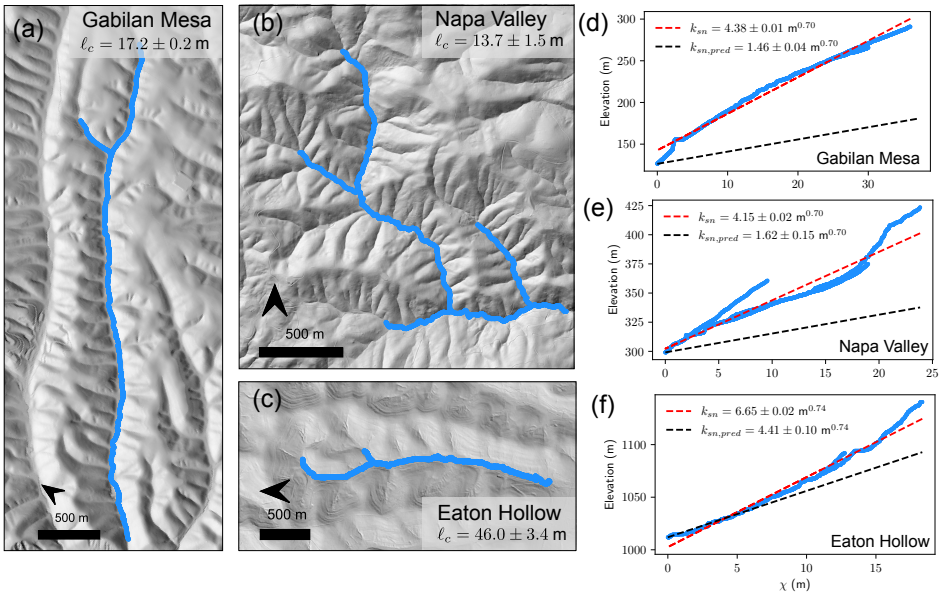

Figure 8. (a, b, c) Hillshades of Gabilan Mesa, California (35.923°N, 120.820°W), Napa Valley, California (38.508°N, 122.332°W), and Eaton Hollow, Pennsylvania (39.904°N, 80.042°W). (d, e, f) χ-elevation profiles for blue channels highlighted in the hillshades. The concavity indices used to calculate χ are 0.35, 0.35, and 0.37 respectively (Perron et al., 2009). The dashed red line is a linear regression, where slope gives an estimate of channel steepness. The dashed black line is the predicted channel profile starting at baselevel and increasing with the steepness predicted by Equation 16.

All three sites have greater channel steepness than would be expected from the 1D SP parameters (Figure 8). Napa Valley has an $\ell_c \approx 14$ m, and a channel steepness deviation $k_{sn}/k_{sn,pred} - 1$ of 1.56. Gabilan Mesa is similar, with $\ell_c \approx 17$ m and steepness deviation of 2.0. Eaton Hollow has the largest value of ℓ_c (46 m), and thus the SPLD scaling predicts the steepness deviation should be largest of the three sites. However, the steepness deviation is only 0.51.

While this is a very limited case study, it does have two important implications. First, channel steepness likely is affected by hillslope sediment, as would be predicted by many models (Sklar and Dietrich, 2006). Second, even in the settings that are supposedly well-suited to the SPLD model, the model is not predictive of channel steepness.

We suggest that the limited steepness deviation at Eaton Hollow could be due to the difference in the character of the hillslope sediment. Eaton Hollow is located on the Appalachian Plateau, which has a lower denudation rate than the other two sites, and thus likely longer regolith residence times, which may lead to production of finer, more easily transportable sediment.

https://doi.org/10.5194/egusphere-2024-2418
Preprint. Discussion started: 15 August 2024

If this is the case, the SPACE model prediction that channel slope reduces to the detachment limited prediction when sediment is easily erodible could be relevant. This hypothesis could be tested by extending the analysis to more sites and including grain size distribution estimates. While the SPACE+diffusion model with high sediment erodibility would predict that channel heads should be much closer to ridges at Eaton Hollow, it is possible that thresholds associated with runoff generation could be important control on drainage density here (Litwin et al., 2022, 2024). This could be further addressed with site-based measurements of the extent of surface runoff.

5 Conclusions

We showed that hillslope diffusion increases channel steepness in 'streampower plus diffusion' (SPD) landscape evolution models. When diffusion is linear (the SPLD model), we showed the steepness can be predicted from the model parameters. The steepness increases directly with diffusivity, and inversely with the grid cell width, when grid cell dependency is not explicitly corrected.

While real rivers are known to steepen to accommodate sediment transport, the particular representation in SPD models are limited to cases where sediment is at once as difficult to suspend as bedrock is to detach, but once suspended, it remains so and is no longer accounted for downstream. This is a consequence of combining a mass conserving model of hillslope processes with a non-mass-conserving model of fluvial erosion, and tracking only a single topographic surface. As a result, the steepness scaling of the SPLD model should have limited applicability in the field. We showed this at three sites where the SPLD model does make the right prediction of first order valley spacing, but does not adequately predict channel steepness. We suggest this is due to a difference in sediment grain size that affects how much channels may have to steepen to transport sediment.

Despite the lack of field applicability, our steepness scaling is a powerful tool for understanding SPLD model behavior. In parts of the parameter space where the steepness scaling effect is expected to greatly affect the results, or when emergent channel properties are particularly important, we recommend against drawing insights from SPD channel profiles and overall relief. Improvements with minimal increased complexity can be made by distinguishing between sediment and bedrock and tracking sediment mass, as in the SPACE model. Future work on hillslope-channel coupling in two-dimensional models should consider incorporating more explicit representation of sediment grain size, as it is a key factor linking the evolution of hillslopes and the development of channel long profile form.

Code and data availability. All code necessary to reproduce our results and make the figures is archived on Zenodo (Litwin, 2024). Topographic data for Eaton Hollow, Napa Valley, and Gabilan Mesa are available from OpenTopography.

Appendix A: SPLD scaling analysis

Litwin et al. (2022) presented a dimensional analysis of Equations 7 and 8 for the case m=1/2, n=1. We generalize this for any values of the exponents m and n. This dimensional analysis follows Theodoratos et al. (2018) in identifying three separate

https://doi.org/10.5194/egusphere-2024-2418
Preprint. Discussion started: 15 August 2024

dimensions in this equation; time T applies to t, height H applies to z, and horizontal length L applies to a, v_0, and the horizontal coordinates x and y. The coefficients in (8) can be rewritten in terms of characteristic height, length, and timescales h_g, ℓ_g, and t_g, such that each term on the right has the same units as the time derivative of elevation, [H/T].

$$\frac{\partial z}{\partial t} = -\frac{h_g^{1-n}\ell_g^{n-m}}{t_g} a^m |\nabla z|^n + \frac{\ell_g^2}{t_g}\nabla^2 z + \frac{h_g}{t_g}, \tag{A1}$$

where we also assign the gradient operator units of [1/L]. A system of equations can be defined by setting the coefficients of the terms in (A1) equal to the coefficients of the terms in (8):

$$\begin{aligned} U &= \frac{h_g}{t_g} \\ D &= \frac{\ell_g^2}{t_g} \\ K v_0^m &= \frac{h_g^{1-n}\ell_g^{n-m}}{t_g}. \end{aligned} \tag{A2}$$

Solving this system, the characteristic scales are the following, for positive exponents m and n:

$$\begin{aligned} t_g &= \left(\frac{D^{n-m}U^{2-2n}}{K^2 v_0^{2m}}\right)^{1/(m+n)} \\ \ell_g &= \left(\frac{D^n U^{1-n}}{K v_0^m}\right)^{1/(m+n)} \\ h_g &= \left(\frac{D^{n-m}U^{2+m-n}}{K^2 v_0^{2m}}\right)^{1/(m+n)}. \end{aligned} \tag{A3}$$

When $m = 1/2$ and $n = 1$ the characteristic scales reduce to those identified by Litwin et al. (2022).

Appendix B: SPLD steepness scaling

The steepness deviation on the vertical axis of subplots in Figure 5 is a modified ratio of the SPLD channel steepness k_{sn} and the steepness predicted from the 1D SP model $k_{sn,pred}$. We can show that this is equal to $(D\widetilde{\nabla^2 z})/U$, by noting that the effective uplift in channels is $U_{eff} = U + D\widetilde{\nabla^2 z}$ and other parameters (n and K) are unchanged:

$$\left(\frac{k_{sn}}{k_{sn,pred}}\right)^n - 1 = \left[\frac{\left(\frac{U_{eff}}{K}\right)^{1/n}}{\left(\frac{U}{K}\right)^{1/n}}\right]^n - 1 \tag{B1}$$

$$= \frac{U_{eff}}{U} - 1 \tag{B2}$$

$$= \frac{U + D\widetilde{\nabla^2 z}}{U} - 1 \tag{B3}$$

$$= \frac{D\widetilde{\nabla^2 z}}{U} \tag{B4}$$

https://doi.org/10.5194/egusphere-2024-2418
Preprint. Discussion started: 15 August 2024

The scaling between the steepness deviation and ℓ_g/v_0 (Figure 4(d)) then implies a scaling between ℓ_g/v_0 and the hilltop curvature in the SPLD model $\nabla^2 z_h = U/D$:

$$\frac{\ell_g}{v_0} \approx \frac{D\widetilde{\nabla^2 z}}{U} \tag{B5}$$

$$\approx \frac{\widetilde{\nabla^2 z}}{\nabla^2 z_h}. \tag{B6}$$

Thus the model predicts that ℓ_g/v_0 is approximately the ratio of channel to hilltop curvature, and thus that channel curvature can also be estimated a priori.

Appendix C: SPACE steady-state solutions

The steady state relationship between slope and area under detachment limited, transport limited, and mixed bedrock-alluvial cases of the SPACE model (without diffusion) are given by Shobe et al. (2017) Equations 40, 44, and 46 respectively. For detachment limited, the solution is:

$$S = \left(\frac{U}{K_r A^m}\right)^{1/n}. \tag{C1}$$

The transport limited solution is:

$$S = \left[\frac{UV}{K_s A^m r} + \frac{U}{K_s A^m}\right]^{1/n}, \tag{C2}$$

where V is the effective settling velocity, and r is the local runoff rate. The mixed bedrock-alluvial solution is the same, except the second appearance of K_s is replaced with K_r:

$$S = \left[\frac{UV}{K_s A^m r} + \frac{U}{K_r A^m}\right]^{1/n}. \tag{C3}$$

The equilibrium sediment thickness for the mixed bedrock-alluvial case is given by Shobe et al. (2017) Equation 47:

$$H = -H^* \log\left[1 - \frac{V}{\frac{K_s r}{K_r} + V}\right], \tag{C4}$$

where H^* is the bed roughness length scale. All simulations shown in Figure 7 have V=5.0 m/yr, r=1 m/yr, and H^*=1.0 m.

Appendix D: SPLD model with bulk density

The steady state SPLD model can be written with bulk density conversions as:

$$0 = -\rho_r K A^m |\nabla z|^n + \rho_s D \nabla^2 z + \rho_r U \tag{D1}$$

https://doi.org/10.5194/egusphere-2024-2418
Preprint. Discussion started: 15 August 2024

Assuming that the streampower term primarily removes bedrock with bulk density ρ_r and hillslope sediment transport applies to regolith with bulk density ρ_s. On hilltops the fluvial term goes to zero:

$$0 = \rho_s D \nabla^2 z_h + \rho_r U, \tag{D2}$$

where $\nabla^2 z_h$ is the hilltop curvature. Eliminating U from (D1) using (D2), we find

$$\rho_r K A^m |\nabla z|^n = \rho_s D \left(\nabla^2 z - \nabla^2 z_h \right), \tag{D3}$$

from which we can derive the equivalent of (15) that explicitly accounts for bulk density:

$$\frac{\rho_s}{\rho_r} \frac{D}{K} A^{-m} = \frac{|\nabla z|}{\nabla^2 z - \nabla^2 z_h}. \tag{D4}$$

Therefore the intercept of the regression between log of area and log of the right hand side of (15) may actually estimate $\frac{\rho_s D}{\rho_r K}$. Multiplying this estimate by the hilltop curvature as we show in Equation 16 gives us U/K without a bulk density prefactor:

$$\frac{\rho_s}{\rho_r} \frac{D}{K} \nabla^2 z_h = \frac{\rho_s D}{\rho_r K} \frac{\rho_r U}{\rho_s D} = \frac{U}{K}. \tag{D5}$$

This suggests that we can get a reasonable estimate of $\frac{U}{K}$ from $\frac{D}{K}$ and hilltop curvature from Perron et al. (2009) without further accounting for bulk density.

Author contributions. D.L. contributed to conceptualization, data curation, formal analysis, investigation, methodology, software, visualization, and writing – original draft preparation. L.M. contributed to conceptualization, supervision, and writing – review and editing. L.S. contributed to conceptualization and writing – review and editing.

Competing interests. The authors declare no competing interests.

Acknowledgements. We thank Jean Braun for useful discussions and his review of an early version of this manuscript.

https://doi.org/10.5194/egusphere-2024-2418
Preprint. Discussion started: 15 August 2024

References

Barnhart, K. R., Glade, R. C., Shobe, C. M., and Tucker, G. E.: terrainbento 1.0: a Python package for multi-model analysis in long-term drainage basin evolution, Geoscientific Model Development Discussions, pp. 1–57, https://doi.org/10.5194/gmd-2018-204, 2018.

Barnhart, K. R., Hutton, E. W. H., Tucker, G. E., Gasparini, N. M., Istanbulluoglu, E., Hobley, D. E. J., Lyons, N. J., Mouchene, M., Nudurupati, S. S., Adams, J. M., and Bandaragoda, C.: Short communication: Landlab v2.0: a software package for Earth surface dynamics, Earth Surface Dynamics, 8, 379–397, https://doi.org/https://doi.org/10.5194/esurf-8-379-2020, publisher: Copernicus GmbH, 2020a.

Barnhart, K. R., Tucker, G. E., Doty, S. G., Glade, R. C., Shobe, C. M., Rossi, M. W., and Hill, M. C.: Projections of Landscape Evolution on a 10,000 Year Timescale With Assessment and Partitioning of Uncertainty Sources, Journal of Geophysical Research: Earth Surface, 125, e2020JF005 795, https://doi.org/https://doi.org/10.1029/2020JF005795, 2020b.

Bonetti, S., Bragg, A. D., and Porporato, A.: On the theory of drainage area for regular and non-regular points, Proceedings of the Royal Society A: Mathematical, Physical and Engineering Sciences, 474, 20170 693, https://doi.org/10.1098/rspa.2017.0693, publisher: Royal Society, 2018.

Bonetti, S., Hooshyar, M., Camporeale, C., and Porporato, A.: Channelization cascade in landscape evolution, Proceedings of the National Academy of Sciences, 117, 1375–1382, https://doi.org/10.1073/pnas.1911817117, publisher: National Academy of Sciences Section: Physical Sciences, 2020.

Bovy, B. and Lange, R.: fastscape-lem/fastscape: Release v0.1.0, https://doi.org/10.5281/ZENODO.8375653, 2023.

Braun, J. and Willett, S. D.: A very efficient O(n), implicit and parallel method to solve the stream power equation governing fluvial incision and landscape evolution, Geomorphology, 180-181, 170–179, https://doi.org/10.1016/j.geomorph.2012.10.008, 2013.

Campforts, B., Schwanghart, W., and Govers, G.: Accurate simulation of transient landscape evolution by eliminating numerical diffusion: the TTLEM 1.0 model, Earth Surface Dynamics, 5, 47–66, https://doi.org/10.5194/esurf-5-47-2017, publisher: Copernicus GmbH, 2017.

Campforts, B., Shobe, C. M., Steer, P., Vanmaercke, M., Lague, D., and Braun, J.: HyLands 1.0: a hybrid landscape evolution model to simulate the impact of landslides and landslide-derived sediment on landscape evolution, Geoscientific Model Development, 13, 3863–3886, https://doi.org/10.5194/gmd-13-3863-2020, publisher: Copernicus GmbH, 2020.

Clubb, F. J., Mudd, S. M., Milodowski, D. T., Hurst, M. D., and Slater, L. J.: Objective extraction of channel heads from high-resolution topographic data, Water Resources Research, 50, 4283–4304, https://doi.org/10.1002/2013WR015167, publisher: John Wiley & Sons, Ltd, 2014.

Egholm, D. L., Knudsen, M. F., and Sandiford, M.: Lifespan of mountain ranges scaled by feedbacks between landsliding and erosion by rivers, Nature, 498, 475–478, https://doi.org/10.1038/nature12218, publisher: Nature Publishing Group, 2013.

Finnegan, N. J., Klier, R. A., Johnstone, S., Pfeiffer, A. M., and Johnson, K.: Field evidence for the control of grain size and sediment supply on steady-state bedrock river channel slopes in a tectonically active setting, Earth Surface Processes and Landforms, 42, 2338–2349, https://doi.org/10.1002/esp.4187, 2017.

Ganti, V., Passalacqua, P., and Foufoula-Georgiou, E.: A sub-grid scale closure for nonlinear hillslope sediment transport models, Journal of Geophysical Research: Earth Surface, 117, https://doi.org/10.1029/2011JF002181, 2012.

Gasparini, N. M., Tucker, G. E., and Bras, R. L.: Network-scale dynamics of grain-size sorting: implications for downstream fining, stream-profile concavity, and drainage basin morphology, Earth Surface Processes and Landforms, 29, 401–421, https://doi.org/10.1002/esp.1031, 2004.

https://doi.org/10.5194/egusphere-2024-2418
Preprint. Discussion started: 15 August 2024

Harel, M. A., Mudd, S. M., and Attal, M.: Global analysis of the stream power law parameters based on worldwide 10Be denudation rates, Geomorphology, 268, 184–196, https://doi.org/10.1016/j.geomorph.2016.05.035, 2016.

Heimsath, A. M., Dietrich, W. E., Nishiizumi, K., Finkel, R. C., Mass, A., and National, L. L.: The Soil Production Function and Landscape Equilibrium, Nature, 388, 358–361, https://doi.org/10.1144/SP312.8, 1997.

Hergarten, S.: Rivers as linear elements in landform evolution models, Earth Surface Dynamics, 8, 367–377, https://doi.org/10.5194/esurf-8-367-2020, publisher: Copernicus GmbH, 2020.

Hergarten, S. and Pietrek, A.: Self-organization of channels and hillslopes in models of fluvial landform evolution and its potential for solving scaling issues, Earth Surface Dynamics, 11, 741–755, https://doi.org/10.5194/esurf-11-741-2023, 2023.

Hobley, D. E. J., Adams, J. M., Nudurupati, S. S., Hutton, E. W. H., Gasparini, N. M., Istanbulluoglu, E., and Tucker, G. E.: Creative computing with Landlab: an open-source toolkit for building, coupling, and exploring two-dimensional numerical models of Earth-surface dynamics, Earth Surface Dynamics, 5, 21–46, https://doi.org/10.5194/esurf-5-21-2017, 2017.

Howard, A. D.: A detachment-limited model of drainage basin evolution, Water Resources Research, 30, 2261–2285, https://doi.org/10.1029/94WR00757, 1994.

Howard, A. D. and Kerby, G.: Channel changes in badlands, GSA Bulletin, 94, 739–752, https://doi.org/10.1130/0016-7606(1983)94<739:CCIB>2.0.CO;2, 1983.

Johnson, J. P. L., Whipple, K. X., Sklar, L. S., and Hanks, T. C.: Transport slopes, sediment cover, and bedrock channel incision in the Henry Mountains, Utah, Journal of Geophysical Research: Earth Surface, 114, 2007JF000 862, https://doi.org/10.1029/2007JF000862, 2009.

Lai, L. S.-H., Roering, J. J., Finnegan, N. J., Dorsey, R. J., and Yen, J.-Y.: Coarse sediment supply sets the slope of bedrock channels in rapidly uplifting terrain: Field and topographic evidence from eastern Taiwan, Earth Surface Processes and Landforms, 46, 2671–2689, https://doi.org/10.1002/esp.5200, 2021.

Lamb, M. P., Finnegan, N. J., Scheingross, J. S., and Sklar, L. S.: New insights into the mechanics of fluvial bedrock erosion through flume experiments and theory, Geomorphology, 244, 33–55, https://doi.org/10.1016/j.geomorph.2015.03.003, 2015.

Litwin, D.: Scripts for "Hillslope diffusion and channel steepness in landscape evolution models", https://doi.org/10.5281/zenodo.13143154, 2024.

Litwin, D. G., Tucker, G. E., Barnhart, K. R., and Harman, C. J.: Groundwater affects the geomorphic and hydrologic properties of coevolved landscapes, Journal of Geophysical Research: Earth Surface, 127, e2021JF006 239, https://doi.org/10.1029/2021JF006239, 2022.

Litwin, D. G., Tucker, G. E., Barnhart, K. R., and Harman, C. J.: Catchment coevolution and the geomorphic origins of variable source area hydrology, Water Resources Research, 60, e2023WR034 647, https://doi.org/10.1029/2023WR034647, 2024.

Lyons, N. J., Val, P., Albert, J. S., Willenbring, J. K., and Gasparini, N. M.: Topographic controls on divide migration, stream capture, and diversification in riverine life, Earth Surface Dynamics, 8, 893–912, https://doi.org/10.5194/esurf-8-893-2020, publisher: Copernicus GmbH, 2020.

Ott, R., Scherler, D., Huppert, K., Braun, J., and Bermudez, M.: Hillslope-controlled incision thresholds shape mountain range topography of the Northern Andes, in: EGU General Assembly 2024, EGU24-2774, Vienna, Austria, https://doi.org/10.5194/egusphere-egu24-2774, 2024, 2024.

Passalacqua, P., Do Trung, T., Foufoula-Georgiou, E., Sapiro, G., and Dietrich, W. E.: A geometric framework for channel network extraction from lidar: Nonlinear diffusion and geodesic paths, Journal of Geophysical Research: Earth Surface, 115, https://doi.org/10.1029/2009JF001254, publisher: John Wiley & Sons, Ltd, 2010.

https://doi.org/10.5194/egusphere-2024-2418
Preprint. Discussion started: 15 August 2024

Pelletier, J. D.: Minimizing the grid-resolution dependence of flow-routing algorithms for geomorphic applications, Geomorphology, 122, 91–98, https://doi.org/10.1016/j.geomorph.2010.06.001, 2010.

Perron, J. T. and Royden, L.: An integral approach to bedrock river profile analysis, Earth Surface Processes and Landforms, 38, 570–576, https://doi.org/https://doi.org/10.1002/esp.3302, 2013.

Perron, J. T., Dietrich, W. E., and Kirchner, J. W.: Controls on the spacing of first-order valleys, Journal of Geophysical Research: Earth Surface, 113, 1–21, https://doi.org/10.1029/2007JF000977, 2008.

Perron, J. T., Kirchner, J. W., and Dietrich, W. E.: Formation of evenly spaced ridges and valleys, Nature, 460, 502–505, https://doi.org/10.1038/nature08174, number: 7254 Publisher: Nature Publishing Group, 2009.

Roering, J. J., Perron, J. T., and Kirchner, J. W.: Functional relationships between denudation and hillslope form and relief, Earth and Planetary Science Letters, 264, 245–258, https://doi.org/10.1016/j.epsl.2007.09.035, 2007.

Roy, S. G., Tucker, G. E., Koons, P. O., Smith, S. M., and Upton, P.: A fault runs through it: Modeling the influence of rock strength and grain-size distribution in a fault-damaged landscape, Journal of Geophysical Research: Earth Surface, 121, 1911–1930, https://doi.org/10.1002/2015JF003662, 2016.

Ruetenik, G. A., Jansen, J. D., Val, P., and Ylä-Mella, L.: Optimising global landscape evolution models with ^{10}Be, Earth Surface Dynamics, 11, 865–880, https://doi.org/10.5194/esurf-11-865-2023, 2023.

Seidl, M. and Dietrich, W. E.: The Problem of Channel Erosion into Bedrock, in: Functional Geomorphology, vol. 23, pp. 101–124, Catena Verlag, Cremlingen-Destedt, Germany, ISBN 3-923381-32-8, 1992.

Shen, H., Lynch, B., Poulsen, C. J., and Yanites, B. J.: A modeling framework (WRF-Landlab) for simulating orogen-scale climate-erosion coupling, Computers & Geosciences, 146, 104 625, https://doi.org/10.1016/j.cageo.2020.104625, 2021.

Shobe, C. M., Tucker, G. E., and Barnhart, K. R.: The SPACE 1.0 model: a Landlab component for 2-D calculation of sediment transport, bedrock erosion, and landscape evolution, Geoscientific Model Development, 10, 4577–4604, https://doi.org/10.5194/gmd-10-4577-2017, 2017.

Sklar, L. S.: Grain Size in Landscapes, Annual Review of Earth and Planetary Sciences, https://doi.org/10.1146/annurev-earth-052623-075856, publisher: Annual Reviews, 2024.

Sklar, L. S. and Dietrich, W. E.: River longitudinal profiles and bedrock incision models: Stream power and the influence of sediment supply, in: Rivers Over Rock: Fluvial processes in Bedrock Channels, vol. 107 of *Geophysical Monograph Series*, pp. 237–260, American Geophysical Union, 1998.

Sklar, L. S. and Dietrich, W. E.: A mechanistic model for river incision into bedrock by saltating bed load, Water Resources Research, 40, https://doi.org/10.1029/2003WR002496, 2004.

Sklar, L. S. and Dietrich, W. E.: The role of sediment in controlling steady-state bedrock channel slope: Implications of the saltation–abrasion incision model, Geomorphology, 82, 58–83, https://doi.org/10.1016/j.geomorph.2005.08.019, 2006.

Theodoratos, N. and Kirchner, J. W.: Dimensional analysis of a landscape evolution model with incision threshold, Earth Surface Dynamics, 8, 505–526, https://doi.org/https://doi.org/10.5194/esurf-8-505-2020, publisher: Copernicus GmbH, 2020.

Theodoratos, N., Seybold, H., and Kirchner, J. W.: Scaling and similarity of a stream-power incision and linear diffusion landscape evolution model, Earth Surface Dynamics, 6, 779–808, https://doi.org/https://doi.org/10.5194/esurf-6-779-2018, publisher: Copernicus GmbH, 2018.

https://doi.org/10.5194/egusphere-2024-2418
Preprint. Discussion started: 15 August 2024

Tucker, G., Lancaster, S., Gasparini, N., and Bras, R.: The Channel-Hillslope Integrated Landscape Development Model (CHILD), in: Landscape Erosion and Evolution Modeling, Springer US, Boston, ISBN 978-1-4615-0575-4, https://doi.org/10.1007/978-1-4615-0575-4_12, 2001.

Turowski, J. M., Rickenmann, D., and Dadson, S. J.: The partitioning of the total sediment load of a river into suspended load and bedload: a review of empirical data, Sedimentology, 57, 1126–1146, https://doi.org/10.1111/j.1365-3091.2009.01140.x, 2010.

Whipple, K. X. and Tucker, G. E.: Dynamics of the stream-power river incision model: Implications for height limits of mountain ranges, landscape response timescales, and research needs, Journal of Geophysical Research: Solid Earth, 104, 17 661–17 674, https://doi.org/10.1029/1999JB900120, 1999.

Wolf, S. G., Huismans, R. S., Braun, J., and Yuan, X.: Topography of mountain belts controlled by rheology and surface processes, Nature, 606, 516–521, https://doi.org/10.1038/s41586-022-04700-6, publisher: Nature Publishing Group, 2022.